



Surgical treatment for shepherd's crook deformity in fibrous dysplasia: THERE IS NO BEST, ONLY BETTER

Jun Wan¹ · Can Zhang¹ · Yu-peng Liu¹ · Hong-bo He¹ 

Received: 21 December 2017 / Accepted: 24 July 2018 / Published online: 6 August 2018
© SICOT aisbl 2018

Abstract

Background The optimal strategy for shepherd's crook deformity correction remains technically challenging. In particular, it is difficult to perform an accurate osteotomy based on the pre-operative correction plan. Moreover, the choice of ideal hardware remains unclear. In addition, when combined with the deformity of knee joint, the sequence of deformity correction is another overlooked factor when making a correction strategy.

Methods From February 2012 to March 2014, we retrospectively examined a cases series in our department involving the creation of three-dimensional (3D) printing osteotomy templates and inner fixation for shepherd's crook deformity in fibrous dysplasia.

Results A total of ten patients of shepherd's crook deformity were enrolled in this study. The neck shaft angle was corrected from a mean value of 88.1° (range, 73–105°) pre-operatively to a mean value of 128.5° (range, 120–135°) post-operatively; no marked loss in the value was observed (mean, 123.7°; range, 115–130°) at the final follow-up. In addition, compared with patients using dynamic hip screw (DHS), longer operation time and additional blood loss were recorded in patients using intramedullary nail (IN). Moreover, after correction of shepherd's crook deformity, two patients were observed more predominant on their pre-existing valgus knee deformity.

Conclusions 3D printing osteotomy templates facilitate the correction of shepherd's crook deformity. Dynamic hip screw (DHS), combined with polymethylmethacrylate (PMMA) augmentation, yields excellent outcomes and ensures easy placement and non-intramedullary manipulation, lower bleeding volume, and reduced operation time. Prior to the correction of shepherd's crook deformity, the mechanical axis of the lower limb should be carefully examined, and any evidence of valgus knee deformity should be addressed in advance.

Keywords Shepherd's crook deformity · Fibrous dysplasia · 3D printing osteotomy template · Hardware · Knee deformity

Introduction

In cases of fibrous dysplasia in the proximal femur, mechanical stress and repeated occult pathological fracture cause deformities such as coxa vara, anteversion of the femoral neck,

anterior bowing, and rotation in the femur shaft, which consequently lead to shepherd's crook deformity [1]. Early surgical intervention was recommended in children with polyostotic fibrous dysplasia due to the aggressive changing pattern of femoral deformity [2, 3].

Curettage and cancellous bone grafting used to be the most common treatment for fibrous dysplasia. However, previous studies have shown that all bone grafts were resorbed and the lesion persisted in these cases; in fact, none of the cases exhibited eradication of size reduction of the lesions [4]. It has become apparent that the most important treatment goal is to correct the deformity, which can provide good mechanical realignment for normal walking ability and pain relief [5].

However, the optimal strategy of deformity correction remains technically challenging [6–10]. In patients with shepherd's crook deformity, it is difficult to accurately perform osteotomy based on the pre-operative correction plan. The

Electronic supplementary material The online version of this article (<https://doi.org/10.1007/s00264-018-4074-9>) contains supplementary material, which is available to authorized users.

✉ Hong-bo He
xiangyahhb@163.com; jonson8920@sina.com

Jun Wan
amiba3000@163.com

¹ Department of Orthopaedics, Xiangya Hospital, Central South University, Xiangya Road 87#, Changsha 410008, Hunan Province, People's Republic of China

success of surgical correction depends on the surgical technique and experience of the surgeons.

Another challenge of surgical correction is the choice of hardware to facilitate the surgery, which should ideally reduce bleeding during the surgery, reduce radiation exposure, and maintain the correction angle [11–13]. Moreover, the sequence of deformity correction is a key factor that is often overlooked in preparing a correction strategy. In patients with polyostotic fibrous dysplasia, both the femur and tibia could be involved. However, previous studies mainly focused on the correction of proximal femur deformity, and few discussed treatments in combination with correction of knee joint deformity such as knee valgus or varus.

In the present study, we performed a retrospective study of case series with surgical intervention for shepherd's crook deformity due to fibrous dysplasia in our department. Accordingly, we sought to address whether three-dimensional (3D) printing osteotomy templates provide more accuracy for deformity correction, which hardware ensures better outcome for deformity correction, and the sequence of deformity correction in cases combined with deformity of the knee.

Materials and methods

This study was conducted in accordance with the declaration of Helsinki and with approval from the ethics committee in our hospital, and informed consent was obtained from all patients regarding the use of their medical information.

From February 2012 to March 2014, a total of ten patients received surgical correction of shepherd's crook deformity due to fibrous dysplasia in our department. The average patient age was 31.2 years (range, 21–38 years; six women and four men). All patients complained of pain in the hip joint and a history of pathological fracture at the proximal femur. Five patients had a history of previous surgery. Prior to the surgery, two presented with valgus knee deformity and three presented with varus knee deformity according to analysis of the mechanical axis of lower limb (Table 1).

Pre-operative planning and manufacturing of 3D printing osteotomy templates

Both the affected and contralateral femurs of patients were scanned using spiral 3D computer tomography (CT), and the data were stored in the DICOM format in a personal computer with the Windows 10 software system. 3D reconstruction of the affected and contralateral femur was performed using Mimics 16.0 software (Materialise, Leuven, Belgium). The angle of the femoral neck shaft, angle of anteversion of the femoral neck, and angle of anterior bowing of the femoral shaft were defined in the software. Using the principles of

Table 1 Patients' demographic and surgical data

Patients number/gender	Age	Side	Times of previous surgery	Hardware	PMMA augmentation	Knee deformity (preoperative)	Operation time (min)	Volume of bleeding (ml)	Secondary deformity after surgery	Complications
1/M	29	R	None	DHS	Yes	None	130	280	None	None
2/F	33	L	1 (curettage and bone grafting)	DHS	Yes	Knee varus	140	300	None	None
3/F	38	L	3 (curettage and bone grafting)	DHS	Yes	Knee varus	160	300	None	None
4/F	34	R	1 (curettage and bone grafting)	DHS	Yes	Knee valgus	178	320	Knee valgus (more predominant)	None
5/F	38	R	None	IN	None	None	390	3300	None	None
6/M	37	L	2 (curettage and bone grafting)	DHS	None	None	220	380	None	None
7/M	21	L	None	DHS	None	None	100	150	None	Translation of femoral shaft (revision surgery needed)
8/F	27	R	1 (curettage and bone grafting)	IN	None	Knee varus	380	6000	None	Wound superficial infection
9/M	24	L	None	IN	None	Knee valgus (mild)	350	2800	Knee valgus (moderate)	None
10/F	31	L	None	DHS	Yes	None	120	300	None	None

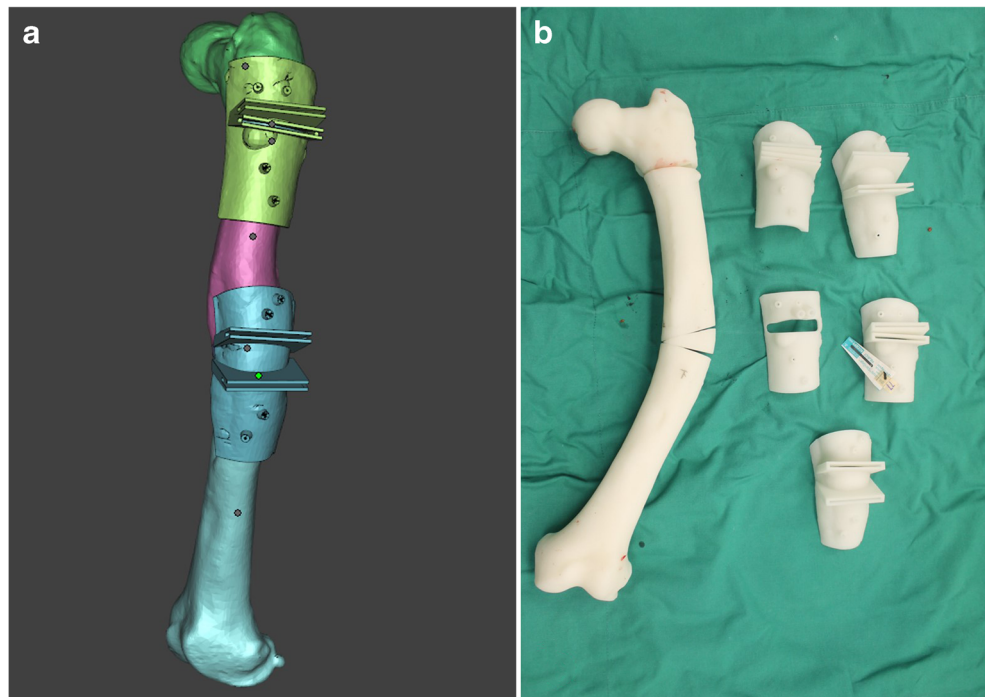
deformity correction, the center of rotation angulation (CORA) was identified, and the osteotomy plan was simulated with the software. Finally, the data of osteotomy template models were exported and printed using nylon polyamides via the rapid prototyping technique (Fig. 1a, b).

Intra-operative surgical technique

The surgical procedure is described as follows. The patient is positioned on a fracture table, and the C-arm fluoro-image intensifier was placed between the patient's legs. A lateral straight incision was made, and the osteotomy template was anchored with k-wires (diameter, 3.5 mm) onto the most suitable surface of the bone, similar to that in the pre-operative plan (Fig. 2a).

Osteotomy was performed using an electric saw along the designed osteotomy line of the template, and the deformity was corrected as indicated in the pre-operative simulated plan (Fig. 2b, c). Care should be taken that the proximal and distal section should not be completely osteotomized and separated. Lesion tissues around the osteotomy site were removed via bony curettage under direct vision. Thereafter, the osteotomy was manipulated and dynamic hip screw (DHS, manufactured by WEGO Medical Limited Company, Shandong, People's Republic of China) or intramedullary nail (IN, manufactured by Stryker Corporation, Michigan, USA) fixation was performed to stabilize the correction. In cases where DHS fixation was chosen, PMMA cement was used to augment the purchase of the screw (Fig. 2d; except in case 7, Table 1).

Fig. 1 **a** Design of 3D printing osteotomy template according to the needed degree of deformity correction. **b** Manufacture of 3D printing osteotomy template by use of the rapid prototyping technique (nylon polyamides as printed material)



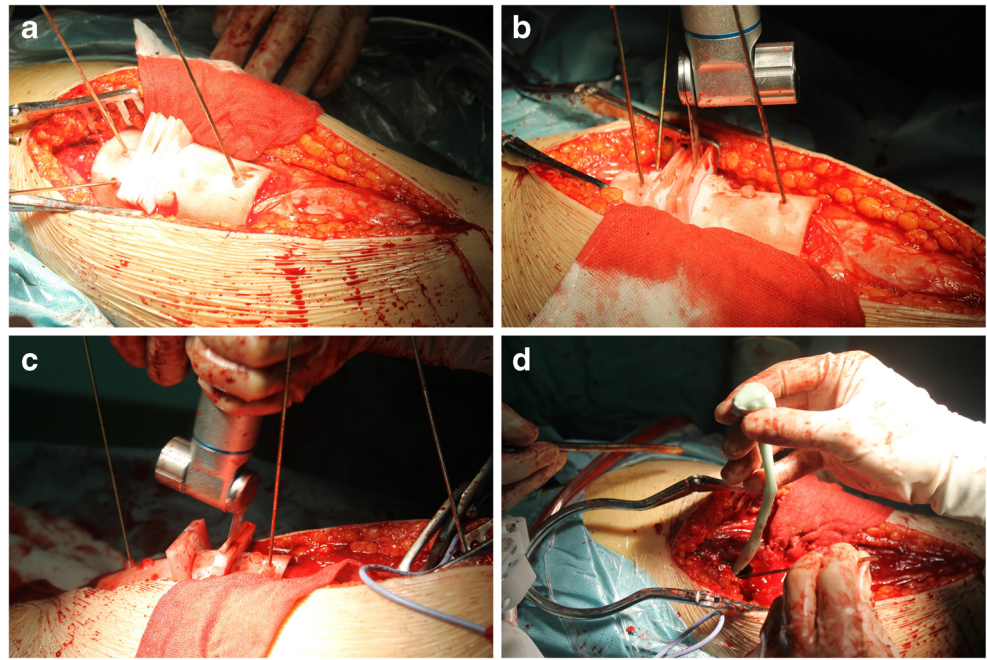
Post-operative treatment

After surgery, patients were allowed to exercise the quadriceps femoris muscle in a long contraction manner and passively move the hip and knee joints 24 hours after surgery. Partial weight-bearing was allowed six to eight weeks after surgery. The time of initiation for full weight-bearing walking was approximately four months. The schedule for follow-up was every three months for the first year and every six months thereafter at the outpatient department. Osteotomy union, neck shaft angle of the femur, and limb length discrepancy were compared on radiological examination pre-operatively and post-operatively. The clinical results were evaluated by a modified criteria presented by Guille et al. [4].

Results

A total of seven patients underwent DHS fixation, and three underwent IN fixation. The mean operation time for the DHS group was 149.7 minutes (range, 100–220 minutes), compared with 373.3 min (range, 350–390 minutes) in the IN group. The mean bleeding volume was 290 ml (range, 150–380 ml) in the DHS group and 4033 ml (range, 2800–6000 ml) in the IN group. All the ten patients were followed up, as mentioned above. The mean follow-up duration was 33.9 months (range, 21–42 months). Osteotomy union was noted in all cases at the final follow-up. The neck shaft angle was corrected from a mean value of 88.1° (range, $73\text{--}105^\circ$) pre-

Fig. 2 Application of 3D osteotomy template during the surgery. **a** Osteotomy template was anchored with k-wires (diameter 3.5 mm) onto the most suitable surface of bone, which is the same as preoperative plan. **b** The osteotomy was made by using an electric saw along with the designed osteotomy line of the template



operatively to a mean value of 128.5° (range, $120\text{--}135^\circ$) post-operatively; no marked loss was observed (mean, 123.7° ; range, $115\text{--}130^\circ$) at the final follow-up. Limb length discrepancy was improved from 3.1 cm (range, 2–3.5 cm) before surgery to 0.6 cm (range, 0–4 cm) at the final follow-up. Interestingly, in cases with varus knee deformity as well, the knee deformities could be corrected simultaneously after correction of shepherd's crook deformity. According to the modified criteria by Guille et al. [4], the average clinical scores improved from 1.4 (range, 1–3) pre-operatively to 8.2 (range, 6–10) post-operatively. The outcomes were classified as excellent in 7, good in 1, and fair in 2. However, knee valgus deformity was more predominant in two cases (cases 4 and 9) after the correction of shepherd's crook deformity (Tables 1, 2, and 3).

Discussion

Fibrous dysplasia—a common benign skeletal lesion—can develop at any skeletal site, with a predilection for the craniofacial bones, ribs, and long bones of the extremities. The condition can be classified into two types based on the bones involved: monostotic type (one bone involved) or polyostotic type (multiple bones involved). Cases with fibrous dysplasia along with cutaneous hyperpigmentation and hyperfunctioning endocrinopathies were considered to have McCune-Albright syndrome [14]. Moreover, cases with polyostotic fibrous dysplasia and intramuscular myxoid tumor were considered to have Mazabraud syndrome [15].

Curettage and bone grafting were used to treat fibrous dysplasia, although studies have since shown that even after curettage and bone grafting, lesion was fulfilled with

Table 2 Clinical results at follow-up

Patients	Neck shaft angle $^\circ$ (pre-op)	Neck-shaft angle $^\circ$ (post-op)	LLD (cm) (preop)	Follow-up (months)	Neck-shaft angle $^\circ$ (last follow-up)	Union of osteotomy	LLD (cm) (last follow-up)
1	90	120	2.5	40	115	Yes	None
2	73	125	3.5	42	122	Yes	None
3	80	120	3	38	116	Yes	None
4	74	135	6	28	130	Yes	4
5	80	130	3	30	126	Yes	None
6	81	130	3	28	124	Yes	None
7	100	125	2	21	120	Yes	None
8	103	135	2	36	130	Yes	None
9	95	135	3.5	38	130	Yes	2
10	105	130	2.5	38	124	Yes	None

Table 3 Clinical scores evaluated by modified criteria of Guille

Categories	Unsatisfactory		Average		Satisfactory	
	Pre-op	Post-op	Pre-op	Post-op	Pre-op	Post-op
Pain	7	0	3	1	0	9
Hip motion	0	0	8	3	2	7
Limping	5	0	5	2	0	8
Activities of daily living	6	0	4	2	0	8
Social activities	7	0	3	2	0	8

Clinical results: 0 (unsatisfactory), 1 (average), 2 (satisfactory); > 9 points defined as excellent, 7–8 points defined as good, 5–6 points defined as fair, < 5 points defined as poor

regeneration tissue of fibrous dysplasia rather than normal bone [4]. In our case series, four patients received curettage and bone grating prior to correction surgery; the same regeneration of fibrous dysplasia was observed in these patients, and as their age increased, the deformity of proximal femur progressively worsened and manifested as shepherd's crook deformity in the end. Ippolito et al. [3] found that the changing pattern of femoral deformity was more aggressive over a seven year follow-up in 46 cases with polyostotic fibrous dysplasia of the femur; they indicated that early surgical intervention should be performed in children with polyostotic fibrous dysplasia.

Studies have found that deformities in this condition not only include coxa vara but also anteversion of the femoral neck and anterior bowing and rotation of the femoral shaft [2, 5]. The complexity of the deformity complicates the intra-operative osteotomy and is also dependent on the subject, which further contributes to the inaccuracy of the surgery.

In recent years, the 3D printing of patient-specific instruments has become more common in pre-operative planning, particularly with regard to surgical templates. Digital 3D reconstruction and reverse modeling technology, combined with 3D printing, could help produce a navigation template for this purpose. 3D printing of osteotomy templates could reduce subject-based errors, including the lack of knowledge of the deformity and poor surgical technique. Moreover, its application could increase the accuracy of the osteotomy, as delineated in the pre-operative plan. Studies have reported tremendous advantages such as reduced operation time, accurate osteotomy angle, and lower radiation exposure [16–19].

In the present case series, due to the complexity of shepherd's crook deformity, the osteotomy plan was created using the Mimics software system in advance; this enabled a 3D and eagle's eye view of the deformity. Thereafter, a 3D printed osteotomy model was designed with software based on the osteotomy plan. The model was designed to suit the irregular shape of the osteotomy site and could be easily used for osteotomy. In cases with femoral shaft rotation, two index bars were designed to facilitate realignment of the shaft. During the surgery, we used the osteotomy template based on the pre-operative plan to achieve easier and more convenient

osteotomy; this ensured that the deformity correction outcome was similar to that determined in the pre-operative plan. In fact, the radiographic outcomes on post-operative follow-up presented the same correction angle, as that noted during the pre-operative plan (Fig. 3a–c).

In fibrous dysplasia of the bone, the abnormal proliferation of fibrous tissue led to a decline in bone strength, which could not provide sufficient control for internal fixation. Therefore, due to the smaller eccentric distance of inner fixation, a shorter force arm, and reduced stress, intramedullary fixation has been advocated theoretically by scholars to maintain the effect of correction and prevent the recurrence of malformations [9]. However, the actual operation was difficult, not cost-effective, and time consuming. First, due to coxa vara, the insertion point of the needle could not be recognized during needle insertion [20]. Second, reaming can lead to the destruction of the lateral wall of the large trochanter and can easily lead to fracture [21, 22]. Finally, due to the presence of a large amount of fibrous tissue in the medullary cavity, it could be difficult to control the direction of reaming [11]. Ippolito et al. [20] preferred two-stage surgery in cases where the entry point was difficult to identify and reaming of the proximal osteotomy fragment was challenging. They indicated the possibility of fracture and injury of the retinacular vessel, which could have led to correction failure and necrosis of the femoral head.

Intra-operative bleeding was another factor to consider. Some studies have found that in cases using IN, massive bleeding may occur when reaming the fibro-dysplastic bone tissue during the surgery [20–22]. In the present case with IN fixation, the volume of bleeding was 2800 ml (case 9), 3300 ml (case 5), and 6000 ml (case 8). In particular, case 8 experienced hypovolemic shock during surgery. Therefore, we do not recommend the use of IN, except in cases where the distal femur needed to be fixed simultaneously.

DHS fixation is another option with the advantages of extramedullary direct vision placement and the absence of the need for intramedullary reaming. Several studies have reported excellent results [13, 23]. However, problems could not be omitted such as cutout of the hardware, screw loosening and pullout, fracture of femoral shaft, and secondary deformity below the plate [9, 20]. In case 7, the loss of correction was

Fig. 3 **a** A 33-year-old woman (case 2) presented severe shepherd's crook deformity. The patients have a second deformity of knee varus with 3-cm low limb discrepancy. 3D printing osteotomy template and 3D printing model of shepherd's crook deformity could be seen in Fig. 1a, b. **b** The needed degree for deformity correction and simulate effect of correction in Mimic 16.0 software. **c** Radiographical outcome in the follow-up. Good alignment of low limb could be observed without discrepancy. Attention should be paid on the simultaneous correction deformity of knee varus without any surgery in the knee joint. (Yellow line as the index of mechanical axis)

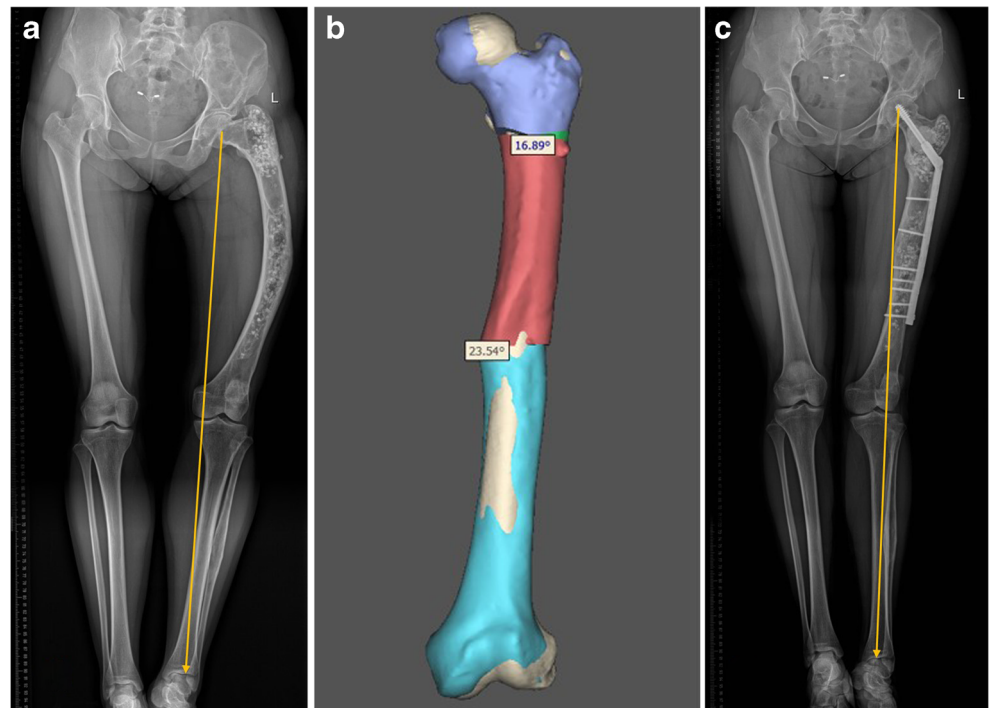


Fig. 4 The post-operative X-ray showed loss of correction in one case (case 7) without PMMA augmentation. He received second revision surgery with PMMA augmentation



observed 2 days after surgery. We believe that when bone cortices were replaced by fibrous bone tissue, its purchase strength was not sufficient, and correction failure was inevitable (Fig. 4a, b). Therefore, we recommend curettage of the proximal lesion and PMMA cement filling in order to merge DHS screw and bone cement into a whole. In this manner, the anti-pullout strength of inner fixation could be markedly increased. In the other cases using DHS in our series, no correction failure was observed when combined with PMMA augmentation.

In cases with shepherd's crook deformity, patients usually exhibited multifocal lesions termed as polyostotic fibrous dysplasia. Hence, it is likely in these cases that another deformity was simultaneously present. Although several studies focused on shepherd's crook deformity, few discussed cases combined with deformity of knee joint. The study by Zhang et al. [9] pointed out if femoral tibial angle was more than 10° , they conducted an additional supracondylar femoral osteotomy. Ippolito et al. [2] recommended to pay attention to the possible worsening of the distal medial bowing or juxtaarticular valgus deformity after correction the shepherd's crook deformity in the proximal femur. However, both of them did not take the mechanical axis of lower limb into account when making correction strategy.

Based on the principle of deformity correction [24, 25], the analysis of the mechanical axis of the lower limb is mandatory prior to the treatment of shepherd's crook deformity. If valgus knee joint deformity was confirmed pre-operatively, then the

correction of the proximal femur would have aggravated the degree of valgus deformity of the knee. This phenomenon was noted in cases 4 and 9, wherein the patients needed addition surgery to correct the deformity by osteotomy in distal femur or proximal tibia (Fig. 5a–c). In these cases, we believe that the valgus deformity of the knee should be corrected first (supplement file 1). If varus deformity of the knee joint is confirmed pre-operatively, the shepherd's crook deformity could be managed first. In cases 2, 3, and 8 in the present series, varus deformity of the knee was observed to be well compensated simultaneously after correction of the shepherd's crook deformity.

The present study had certain limitations. First, the study had a small number of patients and no control group. Thus, a comparative assessment of safety could not be performed between DHS and IN fixation in our clinical cases. Second, there was no consensus regarding the patient's emotional score. Third, although the result of correction appears to be sufficient at the end of the follow-up period in our case series, the outcome should be evaluated over a longer time period; in fact, a minimum five year follow-up is needed to ensure safety.

Conclusions

3D printing osteotomy templates facilitate surgery for correction of shepherd's crook deformity. DHS combined with PMMA augmentation yields excellent outcomes, with the

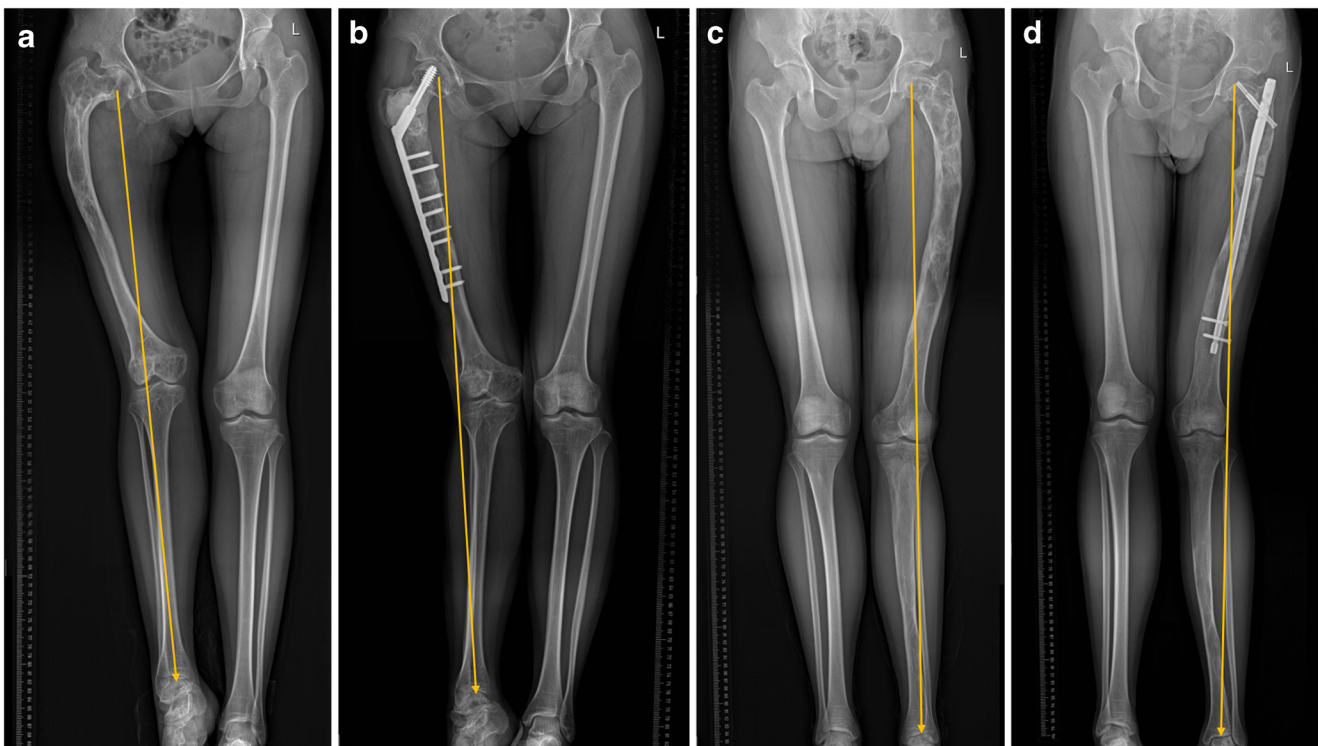


Fig. 5 a–d Two cases of shepherd's crook deformity combined with deformity of knee valgus. Deformity of knee valgus becomes more obvious after correction surgery for shepherd's crook deformity. (a, b for case 4; c, d for case 9; yellow line as the index of mechanical axis)

advantages of easy placement and non-intramedullary manipulation, which reduce the amount of bleeding and operation time, in comparison with IN fixation. Before correcting the shepherd's crook deformity, the mechanical axis of the lower limb should be carefully assessed. If valgus knee deformity is present, it should be corrected in advance.

Acknowledgements We would like to give our sincere thanks to Dr. Qing Liu, Dr. Wei Luo, Dr. Zhan Liao, Dr. Feng Long, and Dr. Jian Tian for data collection and Miss. Jing Wan (the wife of Dr. Jun Wan) for her selfless support during the study.

Funding The study was supported by the National Natural Science Foundation of China (No. 81301671).

Compliance with ethical standards

Conflict of interest The authors declare that they have no conflict of interest.

Ethical approval The study was approved by ethical committee of Xiangya Hospital (document attached as follows).

References

- DiCaprio MR, Enneking WF (2005) Fibrous dysplasia. Pathophysiology, evaluation, and treatment. *J Bone Joint Surg Am* 87:1848–1864
- Ippolito E, Farsetti P, Boyce AM, Corsi A, De Maio F, Collins MT (2014) Radiographic classification of coronal plane femoral deformities in polyostotic fibrous dysplasia. *Clin Orthop Relat Res* 472:1558–1567
- Ippolito E, Valentini MB, Lala R, De Maio F, Sorge R, Farsetti P (2016) Changing pattern of femoral deformity during growth in polyostotic fibrous dysplasia of the bone: an analysis of 46 cases. *J Pediatr Orthop* 36:488–493
- Guille JT, Kumar SJ, MacEwen GD (1998) Fibrous dysplasia of the proximal part of the femur. Long-term results of curettage and bone-grafting and mechanical realignment. *J Bone Joint Surg Am* 80:648–658
- Al-Mouazzen L, Rajakulendran K, Ahad N (2013) Fibrous dysplasia, shepherd's crook deformity and an intra-capsular femoral neck fracture. *Strategies Trauma Limb Reconstr* 8:187–191
- Hagiwara Y, Iwata S, Yonemoto T, Ishii T (2015) Rotational valgus osteotomy for shepherd's crook deformity: a case report. *J Orthop Sci* 20:422–424
- Hefti F, Donnan L, Krieg AH (2017) Treatment of shepherd's crook deformity in patients with polyostotic fibrous dysplasia using a new type of custom made retrograde intramedullary nail: a technical note. *J Child Orthop* 11:64–70
- Watanabe K, Tsuchiya H, Sakurakichi K, Matsubara H, Tomita K (2007) Double-level correction with the Taylor Spatial Frame for shepherd's crook deformity in fibrous dysplasia. *J Orthop Sci* 12:390–394
- Zhang XL, Chen CY, Duan H, Tu CQ (2016) Multiple valgus osteotomies combined with intramedullary nail for shepherd's crook deformity in polyostotic fibrous dysplasia: a case series and review of the literature. *Int J Clin Exp Med* 9:1942–1952
- Sakurakichi K, Tsuchiya H, Yamashiro T, Watanabe K, Matsubara H, Tomita K (2008) Ilizarov technique for correction of the Shepherd's crook deformity: a report of two cases. *J Orthop Surg (Hong Kong)* 16:254–256
- Jung ST, Chung JY, Seo HY, Bae BH, Lim KY (2006) Multiple osteotomies and intramedullary nailing with neck cross-pinning for shepherd's crook deformity in polyostotic fibrous dysplasia: 7 femurs with a minimum of 2 years follow-up. *Acta Orthop* 77:469–473
- Tong Z, Zhang W, Jiao N, Wang K, Chen B, Yang T (2013) Surgical treatment of fibrous dysplasia in the proximal femur. *Exp Ther Med* 5:1355–1358
- Chen WJ, Chen WM, Chiang CC, Huang CK, Chen TH, Lo WH (2005) Shepherd's crook deformity of polyostotic fibrous dysplasia treated with corrective osteotomy and dynamic hip screw. *J Chin Med Assoc* 68:343–346
- Dumitrescu CE, Collins MT (2008) McCune-Albright syndrome. *Orphanet J Rare Dis* 19:12
- Wan J, He HB, Liao QD, Zhang C (2014) An atypical monomelic presentation of Mazabraud syndrome. *Indian J Orthop* 48:429–431
- Honigsmann P, Thieringer F, Steiger R, Haefeli M, Schumacher R, Henning J (2016) A simple 3-dimensional printed aid for a corrective palmar opening wedge osteotomy of the distal radius. *J Hand Surg Am* 41:464–469
- Zhang YZ, Lu S, Chen B, Zhao JM, Liu R, Pei GX (2011) Application of computer-aided design osteotomy template for treatment of cubitus varus deformity in teenagers: a pilot study. *J Shoulder Elb Surg* 20:51–56
- Chen X, Xu L, Wang W, Li X, Sun Y, Politis C (2016) Computer-aided design and manufacturing of surgical templates and their clinical applications: a review. *Expert Rev Med Devices* 13:853–864
- Zheng P, Yao Q, Xu P, Wang L (2017) Application of computer-aided design and 3D-printed navigation template in Locking Compression Pediatric Hip Plate placement for pediatric hip disease. *Int J Comput Assist Radiol Surg* 12:865–871
- Ippolito E, Farsetti P, Valentini MB, Potenza V (2015) Two-stage surgical treatment of complex femoral deformities with severe coxa vara in polyostotic fibrous dysplasia. *J Bone Joint Surg Am* 97:119–125
- Kataria H, Sharma N, Kanojia RK (2009) One-stage osteotomy and fixation using a long proximal femoral nail and fibular graft to correct a severe shepherd's crook deformity in a patient with fibrous dysplasia: a case report. *J Orthop Surg (Hong Kong)* 17:245–247
- Yang L, Jing Y, Hong D, Chong-Qi T (2010) Valgus osteotomy combined with intramedullary nail for Shepherd's crook deformity in fibrous dysplasia: 14 femurs with a minimum of 4 years follow-up. *Arch Orthop Trauma Surg* 130:497–502
- Li W, Huang X, Ye Z, Yang D, Tao H, Lin N, Yang Z (2013) Valgus osteotomy in combination with dynamic hip screw fixation for fibrous dysplasia with shepherd's crook deformity. *Arch Orthop Trauma Surg* 133:147–152
- Paley D, Tetsworth K (1992) Mechanical axis deviation of the lower limbs: preoperative planning of uniapical angular deformities of the tibia or femur. *Clin Orthop Relat Res* 280:48–64
- Paley D, Herzenberg JE, Tetsworth K, McKie J, Bhav A (1994) Deformity planning for frontal and sagittal plane corrective osteotomies. *Orthop Clin North Am* 25:425–465